

Research on Green Soil Slope and Application of Low Carbon Materials

Qisheng Hu¹, Leping He¹, Qijun Hu¹, Yuwei Luo², Jun Wu², Zhaolong Li³, Lei Ding³

¹School of Civil Engineering and Surveying, Southwest Petroleum University, China.

²China Railway Guangzhou Engineering Bureau Group Shenzhen Engineering Co., Ltd, China.

³China Railway 23rd Bureau Group First Engineering Co., Ltd, China.

Abstract

With the promotion of ecological civilization construction and the "dual carbon" goal, the high energy consumption, high carbon emissions, and ecological damage problems of traditional slope engineering urgently need to be solved. This study focuses on the mechanism of stability of green soil slopes and systematically explores the application of low-carbon materials in it. A stability evaluation system for green soil slopes based on low-carbon materials was constructed through literature review, experimental measurement, and numerical analysis. In addition, this study also analyzed the performance characteristics of low-carbon materials and their impact mechanism on slope greening effect and ecological environment. The research results have important theoretical value and practical significance for promoting the low-carbon development of slope ecological maintenance technology and achieving the coordinated progress of engineering construction and ecological protection.

Keywords

Slope Engineering, Stability, Influencing Mechanism, Low carbon Development.

1. Introduction

With the expansion of infrastructure construction scale, the exposed slopes formed by extensive excavation are prone to natural disasters such as landslides and soil erosion, seriously threatening ecological and engineering safety[1]. As the mainstream method of slope ecological restoration, soil spraying technology achieves the dual goals of slope protection and vegetation reconstruction by artificially constructing a substrate layer suitable for plant growth. However, traditional clay materials rely heavily on high energy consuming and costly resources such as cement and peat soil, and the carbon emissions and ecological damage issues generated during their production process are becoming increasingly prominent. Based on the low-carbon materials and functional optimization, this study aims to provide scientific basis and technical support for the construction of green infrastructure by analyzing the impact and evaluation of the stability of green soil slopes.

2. Theoretical analysis of slope stability of guest soil

The weight of the soil is γ , the internal friction angle is c , and the slope angle is α . The soil three-dimensional network interface also satisfies the Mohr Coulomb failure theory, that is, $S_i=c_i+\sigma\tan\varphi$, where the interface cohesion is c_i and the internal friction angle is φ_i [2]. Assuming the thickness of the soil is H , due to the extremely small thickness of the three-dimensional network, it can be ignored. Under the action of gravity, the soil will tend to slide downwards along the sliding surface.

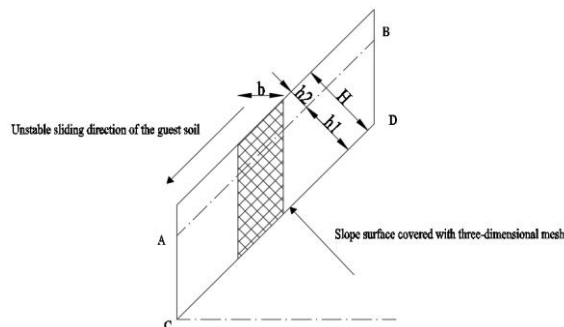


Figure 1 Schematic diagram of soil failure mode and stability analysis

The potential sliding surface is the sliding surface along the three-dimensional mesh surface.

The force analysis of the guest soil unit with a width of b is shown in Figure 2:

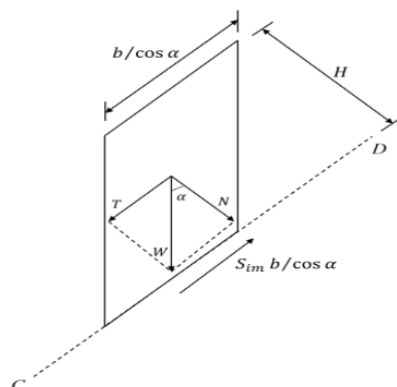


Figure 2 Force diagram of the guest soil unit

The force acting on the guest soil unit is composed of the anti sliding force generated by gravity W and the shear stress S_{im} exerted by the guest soil three-dimensional network interface. The shear stress τ along the slope surface is[3]:

$$\tau = \gamma H \sin \alpha \tag{2-1}$$

The actual shear stress S_{im} exerted by the interface between the guest soil and the 3D mesh is:

$$S_{im} = c_i + \sigma \tan \varphi_i = c_i + \gamma H \cos \alpha \tan \varphi_i \tag{2-2}$$

In the ultimate equilibrium state, the shear stress acting on the sliding element along the slope surface is equal to the shear strength S_i of the soil three-dimensional mesh interface, that is:

$$\tau = S_i \tag{2-3}$$

The critical thickness of the guest soil is:

$$H_{\max} = \frac{c}{\gamma(\sin \alpha - \cos \alpha \cdot \tan \varphi_i)} \tag{2-4}$$

Based on the theoretical analysis of soil stability mentioned above, the design and evaluation of soil stability thickness under the construction method of three-dimensional mesh cushion spraying and grass planting ecological slope protection can be solved.

Assuming a given safety factor of F_s , the stable thickness of the soil in the failure mode is:

$$H_{s1} = \frac{c}{F_s \cdot \gamma(\sin \alpha - \cos \alpha \tan \varphi_i)} \tag{2-5}$$

3. Characteristics of Green Geotechnical 3D Mesh Material

Reinforced three-dimensional geonet pads can be used to improve the stability of vegetation soil on steep rock slopes[4].

Table 1 Three dimensional network performance indicators

	EM2	EM3	EM4	EM5
Material	LLDPE with 0.5%~2.5% (mass fraction) carbon black			
Thickness(mm)	10	12	14	16
Mass per unit area(g/cm ²)	220	260	350	430
Longitudinal tensile strength(kN/m)	0.8	1.6	2.0	3.2
Transverse tensile strength(kN/m)	0.8	1.6	2.0	3.2

Allowable tensile strength of geotechnical three-dimensional mesh[5]:

$$T_a = \frac{T_u}{RF_{CR}RF_{ID}RF_D} = \frac{T_u}{RF} \quad (3-1)$$

In the formula: T_u is the tensile strength of the material, RF is the total reduction factor, RF_{CR} is the failure reduction factor, RF_D is the material aging reduction factor, and RF_{ID} is the creep reduction factor.

The calculation of tensile strength in geotechnical 3D mesh design needs to consider external force components and the strength of flexible materials themselves. Among them, the calculation of force components includes raindrop splashing force, runoff scouring shear force, slope support force, static friction resistance between the three-dimensional mesh bottom and slope surface, and top and guest soil, as well as guest soil pressure. The calculation formula for the tensile strength of a three-dimensional geonet design is [6]:

$$T_d = \frac{T'}{L} = (\gamma d + \gamma_w h + \rho p \mu_d) L (\sin \alpha - \mu \cos \alpha) + \frac{c_1}{c_2} \gamma_w (L + 2h) \rho p x \quad (3-2)$$

In the formula: T_d is the tensile strength of the three-dimensional network design, T' is the tension of the anchor on the three-dimensional network, L is the width of the three-dimensional network, γ is the shear force of runoff per unit area, d is the splashing force of raindrops per unit area, γ_w is the density of water, h is the depth of slope runoff, p is the rainfall intensity, u_d is the velocity of raindrops falling on the ground, and x is the horizontal length of the runoff line. Relationship between allowable and design tensile strength:

$$T_d \leq \frac{T_a}{F_s} = \frac{T_u}{1.45F_s} \quad (3-3)$$

In the formula: F_s is the safety factor.

4. Determination of physical properties of undisturbed soil through testing

In order to better obtain the physical and mechanical properties of the soil in the research area, relevant physical and mechanical tests were conducted on the undisturbed plain soil and root soil composite on site.

4.1. Sampling of test specimens

Four root soil composite ring cutter samples were taken from different locations in the middle of the slope with uniform vegetation coverage, and four plain soil ring cutter samples were taken from the slope without planting preparation. Sampling can be roughly divided into the following steps: ① Clearing vegetation and humus → ② Pressing in with a ring knife → ③ Wrapping and numbering with plastic wrap.



(a)Clean up humus soil (b)Ring knife pressed in (c)Sampling and numbering
Figure 3 Sampling process of intact ring knife

4.2. Physical Properties

The diameter of the soil sample is 61.8mm, the height is 20.0mm, and the bottom area is 30cm². Conduct relevant indoor tests in accordance with the "Standard for Soil Test Methods". The natural density and dry density of soil samples are measured using the ring knife method, the moisture content of soil samples is measured using the drying method, and the liquid limit and plastic limit of soil are measured using the cone meter method[7].



(a)Electric heating blast drying oven (b)Electronic scale (c)Cone meter
Figure 4 Relevant experimental equipment

Table 2 Basic Physical Properties of Natural Soil

index	Natural moisture content (%)	Dry density (g/cm ³)	Liquid limit	Plastic Limit	Liquid Limit Index	Plastic limit index
value	13.718	1.499	26.88	17.8	0.43	0.24

Root content is an important indicator for measuring the physical and mechanical properties of root soil composites. Scholars at home and abroad use different quantitative indicators to characterize it, such as root biomass (RB, total mass of root system per unit of soil, g/cm³) and root cross-sectional area ratio (RAR, the ratio of the sum of root cross-sectional areas affected by shear planes to the soil cross-sectional area). Measure the RAR value of the sample using equation (4-1)[8] [9].

$$RAR = \frac{A_r}{A_s} \times 100\% = \frac{V_r / h}{0.25 \cdot \pi \cdot d^2} \times 100\% = \frac{4V_r}{\pi \cdot d^2 \cdot h} \times 100\% \quad (4-1)$$

In the formula, A_r is the sum of the cross-sectional areas of the root system on the horizontal cross-section of the sample, A_s is the horizontal cross-sectional area of the sample, and d is the radius of the sample.

Table 3 Basic physical properties of root-soil complex

index	Natural moisture content (%)	Natural density (g/cm ³)	Dry density (g/cm ³)	Root content (%)
value	15.252	1.68	1.457	1.83

5. Analysis of factors affecting the stability of the 5 guest soil

5.1. Criteria for soil instability

The instability of the soil can be divided into overall instability and local instability. Overall instability refers to the situation where the sliding force along the slope caused by the overall weight of the soil and the three-dimensional geonet exceeds the tensile capacity of the geonet, leading to its rupture at a certain point. Local instability includes two situations. Firstly, when the downward sliding force along the slope caused by the weight of the soil exceeds the interfacial friction between the soil and the three-dimensional geogrid, the soil will slide along the surface of the geogrid; The second refers to soil that exceeds the influence range of the three-dimensional geogrid. When the force of its own gravity along the slope surface is greater than the shear strength, the soil will undergo local shear failure.

5.2. Analysis of soil damage

Based on FLAC 3D finite difference software, the displacement cloud maps of different soil thicknesses with a slope of 60° are shown in Figure 5. Analysis shows that the displacement of the soil along the slope is characterized by a large displacement in the middle of the slope and a small displacement at the foot and top of the slope. The maximum displacement is 3.47mm and 10.63mm when the thickness of the soil is 10 and 20cm, respectively.

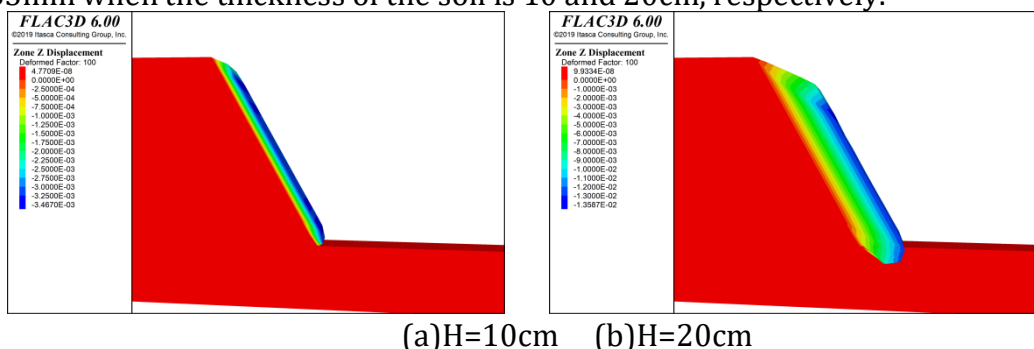


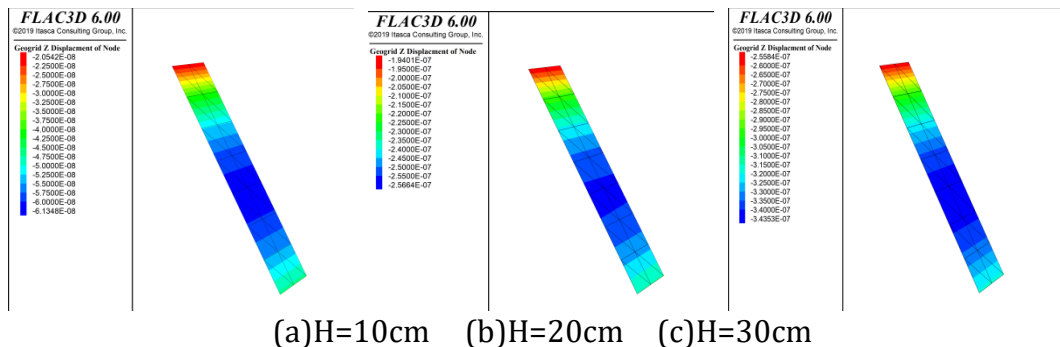
Figure 5 Displacement cloud map of different soil thicknesses with a slope of 60° (magnification factor of 100)

Analysis shows that the larger the slope, the smaller the thickness of the soil when the numerical calculation does not converge, that is, the steeper the slope, the smaller the thickness when it becomes unstable.

Table 4 Summary of Maximum Displacement

thickness \ slope	Maximum displacement along the slope surface/mm						
	10	15	20	25	27.5	30	40
45	1.85	3.71	7.81	13.33	17.2	18.74	Instability
50	2.95	5.52	9.27	14.58	19.01	Instability	--
55	3.02	6.07	10.54	17.28	18.32	Instability	--
60	3.47	7.71	13.59	18.50	Instability	--	--
65	5.47	9.71	17.25	Instability	--	--	--

Figure 6 shows the three-dimensional network displacement cloud map along the slope direction for different soil thicknesses with different slopes. At different thicknesses, the displacement distribution of the three-dimensional network along the slope direction is the same. The displacement of the three-dimensional network is the largest near the bottom in the middle of the slope, and the displacement is the smallest at the top of the slope. The displacement increases with the increase of soil thickness.



(a)H=10cm (b)H=20cm (c)H=30cm
Figure 6 Three dimensional displacement cloud map

Analysis shows that under the same thickness of soil, as the slope gradient increases, the tension of the grid increases. In actual soil spraying, higher specification three-dimensional mesh should be used for steep slopes.

Table 5 Summary of maximum displacement of grating (three-dimensional mesh) along the slope under different working conditions

thickness slope	Maximum displacement along the slope surface/mm						
	10	15	20	25	27.5	30	40
45	0.35	1.28	2.53	2.97	3.02	3.63	Instability
50	0.53	1.55	2.75	3.16	3.97	Instability	--
55	0.57	1.89	2.57	3.84	4.28	Instability	--
60	0.61	2.57	3.44	4.98	Instability	--	--
65	1.58	2.99	5.17	Instability	--	--	--

6. Conclusion

Conducting research on key technologies for green slope design and replacing some traditional steel bars and cement reinforced slopes with green vegetation can save resources to the maximum extent and reduce environmental impact. At the same time, conducting research on green construction technology, developing new technologies, new materials, and new processes, and promoting application demonstration projects can directly achieve economic, social benefits and engineering results.

- (1) Application of green slope design and construction technology to save land and stone resources to the maximum extent, increase green vegetation area, reduce the negative impact of construction activities on the environment, and reduce soil erosion;
- (2) The comprehensive cost of mesh-mounted mud-sprayed green slope is 3% lower than that of commonly used mesh-mounted cement slurry-sprayed slope, and the comprehensive cost of reinforced soil slope (retaining wall) is 3% lower than that of commonly used concrete retaining wall;
- (3) The green slope is stable and reliable, and its anti-erosion capacity is 10% higher than that of the commonly used fill slope treatment method.

Acknowledgments

This work was supported by the National Natural Science Foundation of China (No. U23A2046), the Sichuan Youth Sci-Tech Innovation Team Project (No. 2022JDTD0007), the Tianfu Ten Thousand Talents Program of Sichuan Province (No. 6580), and the Scientific Research Program Projects of China Railway Construction Corporation Limited (CRCC) (No. 2023-Q04).

References

- [1] Li Dongsheng. Optimization process of ecological slope protection matrix for highway rock slope [J]. Shanxi Architecture, 2011, 37 (32): 135-136.
- [2] Yang Junjie, Wang Liang, Zheng Jianguo, Xu Guohui, Wu Yanlin, Wang Xinqiang. Study on stability of imported soil in ecological slope[J]. Chinese Journal of Rock Mechanics and Engineering, 2006, (02): 414-422.
- [3] Wang Liang, Yang Junjie, Liu Qiang, Jia Yonggang, Shan Hongxian, Sun Tianlei. Study on the influence of surface seepage on the stability of imported soil in ecological slope[J]. Rock and Soil Mechanics, 2008, (06): 1440-1445+1450.
- [4] Lu Tao. Experimental and numerical simulation study on stability of vegetation layer of rock slope anchor-geotextile mat spraying grass ecological slope protection[D]. Qingdao University of Technology, 2015.
- [5] Xiao Henglin, Wang Zhao, Zhang Jinfeng. Research on design indexes of three-dimensional geogrids[J]. Rock and Soil Mechanics, 2004, (11): 1800-1804.
- [6] Wang Yun. Overall stability analysis of geotechnical three-dimensional mesh protection slope[D]. Shandong University, 2016.
- [7] Ouyang Huimin. Study on the relationship between microstructural characteristics and macroscopic mechanical properties of soil in the hydraulic filling site of Tianjin Binhai New Area[D]. Tianjin Institute of Urban Construction, 2008.
- [8] Xia Zhenyao, Zhou Zhengjun, Huang Xiaole, Xu Wennian. Preliminary study on the relationship between shallow soil fixation and fractal characteristics of vegetation slope protection roots[J]. Chinese Journal of Rock Mechanics and Engineering, 2011, 30 (S2): 3641-3647.
- [9] Li Mouming. Research on root-soil complex strength model in different growth periods and its application[D]. Central South University of Forestry and Technology, 2022.